Proceedings of the 8th International Symposium on Cavitation
CAV2012 – Submission No. 189
August 13-16, 2012, Singapore

Numerical simulation of 3D self-organization of bubbles in acoustic fields

Nail A. Gumerov
Institute for Advanced Computer Studies,
University of Maryland, College Park, USA;
Center for Micro- and Nanoscale Dynamics of Dispersed Systems,
Bashkir State University, Ufa, Russia

Iskander Sh. Akhatov
Department of Mechanical Engineering,
North Dakota State University, Fargo, USA;
Center for Micro- and Nanoscale Dynamics of Dispersed Systems,
Bashkir State University, Ufa, Russia

SUMMARY

A phenomenon of bubble self-organization also known as structure formation and related self-action of the acoustic field is a strongly non-linear effect, which is observed, e.g. in acoustic cavitation and sonochemical reactors. It is due to a two-way field-particle interaction, when the bubbles change their position and sizes due to the acoustic radiation and other forces and rectified diffusion; so the acoustic properties of the medium vary in space in time, which leads to restructuring of the acoustic field. Mathematical models of this phenomenon available in the literature are studied in very simplified settings, while extensive numerical simulations in three dimensions were not performed. In the present study we provide a basic closed model of equations of self-organization and estimations of the characteristic scales for relatively small amplitude acoustic fields and diluted bubbly liquids. In this case the evolution of a time-harmonic acoustic field occurs in a slow time scale. Bubble drift due to the radiation forces as well as the effect of rectified diffusion can be brought to the same slow time scale for weakly non-linear bubble oscillations. Despite for acoustic cavitation such simplification seems is not valid it allows one to obtain a closed system of equations with clear physical meaning and investigate this system analytically and numerically to get insight to a complex phenomenon. In the present study 2D and 3D codes for simulation of bubble self-organization are developed and tested. Peudospectral iterative solvers for the Helmholtz equation with spatially non-uniform wavenumber are in the core of these codes. Two schemes for temporal evolution were tested and compared; first, fully pseudospectral, and, second, based on the particle (Lagrangian) methods. Simulations show interesting spatio-temporal behavior of the bubbles and the acoustic field, which is generated by a source inside a sound hard box. Particularly effects of bubble clustering, filamentation, etc., observed in acoustic cavitation experiments were also found numerically. Bubble pattern formation is sensitive to many parameters including parameters of the acoustic field, bubble initial size, number density, spatial distribution, and ambient conditions. The effects found in the result of simulations are discussed.

INTRODUCTION

Early studies of self-organization include a paper of Kobelev & Ostrovsky (1989) [1], who proposed a mathematical model which phenolmenologically takes into account dissipation and bubble drift due to the Bjerknes, Stokes, added mass and buoyancy forces. One dimensional planar solutions were studied there. Two-dimensional simulations were performed in studies of Akhatov *et al* (1994, 1996) [2, 3]. The unsteady 'dancing' structures observed in experiments and formation of fractal structures is explained by the same group of authors (Parlitz *et al*, 1995) [4] as an effect of the secondary Bjerknes force acting between bubbles. Gumerov (1998) [5] extended the model to include the effect of rectified diffusion. Only theoretical possibility of realization of soliton-like spatial structures and one dimensional simulations of steady cavitation zone were performed there.

Experimental studies, however, show that three dimensional effects are substantial for the problem considered, and efficient numerical algorithms and 3D simulation tools are needed to understand this complex phenomenon. Development of such tools and estimations of characteristic parameter range is the main purpose of the present study.

MODEL

In the present study we limit ourselves with a weekly nonlinear model of acoustic wave propagation in diluted monodisperse bubbly liquids with spherical bubbles (e.g. Nigmatulin, 1991 [6]). Acoustic waves of relative amplitude $\varepsilon << 1$ and circular frequency ω cause small radial oscillations of bubbles of average radius a_0:

$$\begin{aligned} &p = p_*\left(1+\varepsilon p_1+\ldots\right), \quad a = a_0\left(1+\varepsilon a_1+\ldots\right), \\ &p_1 = \mathrm{Re}\left\{Ae^{-i\omega t}\right\}, \quad a_1 = \mathrm{Re}\left\{-\Lambda\left(a_0\right)Ae^{-i\omega t}\right\}, \end{aligned} \tag{1}$$

where A is the complex amplitude of the field, and Λ is the bubble response function, which for given thermo-physical

properties of the liquid and gas and frequency is a function of the mean bubble radius,

$$\Lambda = \frac{a_0^2}{a_r^2 - a_0^2 - i\eta}, \quad a_r^2 = \frac{3\gamma p_*}{\omega^2 \rho_l}, \tag{2}$$

where a_r is the resonance radius, ρ_l is the liquid density, and $\gamma(a_0)$ and $\eta(a_0)$ are the effective adiabatic exponent and dissipation coefficient. Expressions for these functions can be found in Commander & Prosperetti, 1989 [7] (see also [5]), which include thermal effects and effects of liquid viscosity and acoustic radiation. The cited paper is dedicated to linear waves in bubbly liquids and following the derivation of the dispersion relations, one can find that the amplitude of these waves can be described by the Helmholtz equation

$$\nabla^2 A + k^2 A = 0, \tag{3}$$

where the complex wavenumber, k, can be determined as

$$k^2 = k_l^2 + k_b^2, \quad k_l^2 = \frac{\omega^2}{C_l^2}, \quad k_b^2 = \frac{4\pi\omega^2\rho_l}{p_*} n_0 a_0^3 \Lambda(a_0). \tag{4}$$

Here ρ_l and C_l are the liquid density and speed of sound, while n_0 is the averaged number density of bubbles.

It is noticeable, that equations (1)-(4) hold for spatially non-uniform mixtures, means n_0 and a_0 can be arbitrary functions of spatial coordinate, **x**. It is also allowed for these parameters to be functions of a slow time, means vary in the scale slower than ω^{-1}. To find this scale we consider period-averaged momentum conservation equation, which describes a drift of the bubble in an acoustic field

$$\frac{2}{3}\pi\rho_l \frac{d\langle a^3 \mathbf{v}_b \rangle}{dt} = -\frac{4}{3}\pi \langle a^3 (\nabla p + \rho_l \mathbf{g}) \rangle - 12\pi k_\mu \mu_l \langle a \mathbf{v}_b \rangle. \tag{5}$$

Here $\mathbf{v}_b$ is the bubble velocity. In the left hand side we have the added mass force, while the right hand side present the Bjerknes, gravity, and viscous drag forces; k_μ is the drag coefficient which may take value between 1 (high Reynolds numbers of the relative bubble motion) and 1/3 (low Reynolds numbers). The Stokes drag for a rigid sphere corresponds to k_μ =1/2. In this equation the mass of the gas is neglected compared to the added mass of the liquid. For small oscillations (1) Eq. (5) can be rewritten in the form

$$\frac{d\mathbf{v}_{b0}}{dt} = \frac{3p_*\varepsilon^2}{\rho_l} \mathrm{Re}\{\Lambda A \nabla \overline{A}\} - 2\mathbf{g} - \left[\frac{18 k_\mu \mu_l}{\rho_l a_0^2} + \frac{3}{a_0^2}\frac{da_0}{dt}\right]\mathbf{v}_{b0}, \tag{6}$$

where $\mathbf{v}_{b0}$ is the period-averaged bubble velocity and the bar denotes the complex conjugate.

Equation (6) can be used to determine the period-averaged bubble position in the acoustic field, $\mathbf{x}_{b0}$, or the mean bubble number density, if consider bubbles as a continuum:

$$\frac{d\mathbf{x}_{b0}}{dt} = \mathbf{v}_{b0}, \quad \frac{\partial n_0}{\partial t} + \nabla \cdot (n_0 \mathbf{v}_{b0}) = 0. \tag{7}$$

Equations (6) and (7) also can be used to determine the slow time scale. Neglecting all forces except the Bjerknes force and using the length scale for the bubble position ~ $|k|^{-1}$, we can determine the characteristic time, t_{s*}, during which the bubble migrates in the acoustic field, when the amplitude changes substantially (e.g. between the nodes and antinodes). Assuming $|\Lambda| \sim |A| \sim 1$, $|\nabla A| \sim |k|$ one can get

$$t_{s*} \sim \sqrt{\frac{|k|^{-1}}{|d\mathbf{v}_{b0}/dt|}} \sim \frac{1}{|k|\varepsilon}\sqrt{\frac{\rho_l}{p_*}} \sim \frac{C_*}{\omega\varepsilon}\sqrt{\frac{\rho_l}{p_*}}, \tag{8}$$

where C_* is the characteristic sound speed. Note then that in the case of very low void fractions, α, we have $C_* \sim C_l >> (p_*/\rho_l)^{1/2}$ and in the case of bubble concentration affecting the speed of sound $C_* \sim (p_*/\rho_l\alpha)^{1/2} >> (p_*/\rho_l)^{1/2}$, since anyway we consider diluted mixtures, α <<1. This shows that even for waves of moderate amplitude, $\varepsilon \sim 1$, we have $t_{s*} >> \omega^{-1}$, and t_{s*} becomes much larger for $\varepsilon << 1$.

In fact, this time can be substantially larger if we take into account viscous relaxation. As follows from Eq. (6) the viscous relaxation time is

$$\tau_\mu = \frac{\rho_l a_0^2}{18 k_\mu \mu_l}, \tag{9}$$

which can be much smaller than t_{s*}. For example, for water at atmospheric pressure, bubbles of typical size $a_0 \sim 10^{-4}$ m, and acoustic field $\omega \sim 10^5$ rad/s, $C_* \sim 10^3$ m/s, $\varepsilon \sim 0.1$, we have $t_{s*} \sim 10^{-2}$ s and $\tau_\mu \sim 10^{-3}$ s. On the other hand, the speed of sound in bubbly liquids can be much smaller (especially for bubbles about the resonance size), so if $C_* \sim 10^2$ m/s, then $t_{s*} \sim \tau_\mu$. Situations when $t_{s*} << \tau_\mu$ should not be excluded as well. Anyway, if the viscous relaxation plays a substantial role, then the characteristic drift velocity can be found by balancing of the Bjerknes and viscous forces, which provides the following characteristic velocity and time scales

$$v_{b0*} \sim \frac{\varepsilon^2 p_* \omega \tau_\mu}{\rho_l C_*}, \quad t_{\mu s*} \sim \frac{1}{|k| v_{b0*}} \sim \frac{\rho_l C_*^2}{\varepsilon^2 p_* \omega^2 \tau_\mu}. \tag{10}$$

Note that for the example case with $C_* \sim 10^3$ m/s we have $t_{\mu s*} \sim 10^{-1}$ s >> t_{s*}., $v_{b0*} \sim 10^{-1}$ m/s, while for $C_* \sim 10^2$ m/s we have $t_{\mu s*} \sim 10^{-3}$ s ~ t_{s*}, $v_{b0*} \sim 1$ m/s. In any case these estimates show that $\omega t_{\mu s*}$ >>1 and prove that the slow time scale exists.

Finally, we consider effect of rectified diffusion which also occurs in a slow time scale. This equation was obtained and analyzed by many authors and Crum and Hansen (1982) [8] as well as Fyrillas and Szeri (1994) [9] provide reviews and insight to this phenomenon. For small amplitude stationary oscillations this equation can be written in the form (see [5])

$$\frac{da_0}{dt} = \frac{v_D}{a_0}\left[q(a_0)|A|^2 - s(a_0)\right], \quad v_D = \frac{\varepsilon^2 c_* \rho_l D_l}{\rho_{g^*}},$$
$$q = 6\gamma\left(1 - \frac{a_0^2}{8a_r^2}\right)|\Lambda|^2, \quad s = \frac{1}{\varepsilon^2}\left(\frac{2\sigma}{p_* a_0} - \frac{c_\infty - c_*}{c_*}\right), \tag{11}$$

where σ and D_l are the surface tension and liquid mass diffusivity, c_∞ is the mass concentrations of dissolved gas in the bulk of the liquid, and c_* and ρ_{g^*} are the equilibrium concentration and gas density at pressure p_* and ambient temperature. Note here that the term in the parentheses in s which drives diffusion in the absence of the acoustic field is assumed to be of the order of ε^2, so $s \sim 1$. Indeed, if the right hand side of the first equation (11) is zero, this determines the cavitation threshold and the stationary radius, which for small amplitude waves are of the order of the resonance radius, and, in fact the processes we consider are for the radii of this order.

It is not difficult to estimate the characteristic time of the mean bubble radius change based on this equation. For the example system considered above at $\varepsilon = 0.1$we have $\nu_D \sim 5\cdot 10^{-13}$ m^2/s, which means that if the terms in the square brackets in Eq. (11) are of the order of 1, the time of characteristic change of a_0 is $t_{as^*} \sim a_0^2/\nu_D \sim 10^4$ s. Even if we consider oscillations near the resonance, where q can be, say, $\sim 10^2$, we obtain $t_{as^*} \sim 10^2$ s, which is huge compared to the times of bubble drift estimated above. So, it seems that one can neglect the effect of rectified diffusion at all. However, there are two basic assumptions, which were used in derivation of Eq. (11) and which are violated in the case of self-organization.

The first assumption is that the period-averaged concentration profile around the bubble is quasisteady, means the times considered are $t_* >> a_0^2/D_l \sim 5$ s (for the example case considered). Certainly, this is not true for characteristic drift times t_{us^*}, estimated as $10^{-3} - 10^{-1}$ s. The transient effects were included in some equations (e.g. see [8]) and may cause an order of magnitude or so increase the bubble growth rate.

The second assumption, which seems is more important, is that equations for rectified diffusion are derived for bubbles in isotropic acoustic fields, i.e. for bubbles without translational motion. This effect is not difficult to estimate, since the characteristic diffusion Peclet numbers in the example case considered are of the order $Pe_{D*} = 2a_0 v_{b0*}/D_l \sim 10^4 - 10^5$ (see estimates after Eq. (10)). Roughly speaking, this may intensify the mass transfer $\sim (Pe_{D*})^{1/2}$ times and for some cases bring the effect of rectified diffusion to the scale comparable with the effect of the bubble drift (in fact, for the bubbles of nearly resonance size even smaller intensification of the mass transfer may have a strong effect, since the transition through the resonance size, changes the sign of the Bjerknes force).

A reasonable modeling approximation for these effects can be suggested using results available in literature. For this purpose, we note first that in acoustic waves the characteristic radial velocities of the pulsating bubble $v_{rf^*} \sim \varepsilon\omega a_0$ are usually much larger than the characteristic relative translational velocity oscillations $v_{tf^*} \sim \varepsilon p_*/(\rho_l C_*)$ (e.g. for the example case considered $v_{tf^*}/v_{rf^*} \sim 10^{-2} << 1$, $C_* \sim 10^3$ m/s). Hence the period-averaged gas pressure and surface concentration can be computed as for an isotropic acoustic field, Eq. (11), which provides cavitation threshold $|A|^2 = s/q$ that agrees well enough with experiments even at $\varepsilon \sim 1$ (see [5]). Equation (11) then can be rewritten in the form

$$2a_0 \frac{da_0}{dt} = D_l Nu_D Ja_D, \quad Ja_D = \frac{\varepsilon^2 c_* \rho_l}{\rho_{g^*}}\left(q|A|^2 - s\right), \tag{12}$$

where Nu_D and Ja_D are the diffusional Nusselt and Jacob numbers. Analytical results for the Nusselt number of a bubble of variable radius in a time-dependent potential flow (see Gumerov (1996) [10]). It appears then that in our case we have small Jacob, high Peclet, and small Strouhal numbers, $St = 2a_0/(v_{b0*}t_{s*}) \sim |k|a_0 << 1$. Despite an expression for the transient Nusselt number is available, it was obtained assuming, Ja_D =const for a sudden jump of surface concentration at $t = 0$. More accurate accounting for the transient then should include a prehistory term. In the present paper we drop all these transients to ease the initial mathematical modeling as their role at high Peclet numbers diminishes. An appropriate expression then can be simply reduced to the Levich (1959) [11] formula, to which we add a small term to have $Nu_D = 2$ at zero Peclet numbers, which provides matching with Eq. (11)

$$Nu_D = 2 + \frac{2}{\pi^{1/2}} Pe_D^{1/2}, \quad Pe_D = \frac{2a_0|\mathbf{v}_{b0}|}{D_l}. \tag{13}$$

This closes the model of self-organization, which as a summary can be written in the form enabling continuum description

$$\nabla^2 A + k^2 A = 0, \quad k^2 = k^2(n_0, a_0),$$
$$\frac{d_b n_0}{dt} = -n_0 \nabla\cdot\mathbf{v}_{b0}, \quad \frac{d_b a_0}{dt} = Q(a_0, \mathbf{v}_{b0}, |A|^2), \tag{14}$$
$$\frac{d_b \mathbf{v}_{b0}}{dt} = \mathbf{F}\left(a_0, \mathbf{v}_{b0}, |A|^2\right), \quad \frac{d_b}{dt} = \frac{\partial}{\partial t} + \mathbf{v}_{b0}\cdot\nabla.$$

METHODS OF SOLUTION

From computational point of view most challenges are related to solution of the elliptic Helmholtz equation with spatially non-uniform k. We developed and tested a pseudospectral solver for this equation, which in future can be replaced by another solver that can handle more complex geometries and model realistic experimental conditions.

All computations of the present paper are performed for a point source of sound placed at the center of $L_1\times L_2\times L_3$ box B with rigid walls. The normal derivative of pressure on such walls is 0, $\partial p/\partial n = 0$, which can be simply forced by imposing periodic boundary conditions and symmetry of the solution with respect to each wall. If the origin of the reference frame is placed to the box center we have

$$f(x_j + L_j) = f(x_j) = f(-x_j), \quad f = A, k, \quad j = 1,2,3, \tag{15}$$

where x_j are Cartesian coordinates of point $\mathbf{x}$, and f refers both to the complex amplitude and wavenumber. Then for a unit source and given $k^2(\mathbf{x})$ we solve for $\mathbf{x}$ located in the box

$$\nabla^2 A + k^2 A = -\delta_d(\mathbf{x}), \quad \delta_d = \frac{1}{(d\sqrt{\pi})^3} e^{-|\mathbf{x}|^2/d^2}, \qquad (16)$$

where δ_δ is an approximation of the Dirac's delta-function, which we use to avoid singular values at the origin. All functions then are sampled on a regular grid $N_1 \times N_2 \times N_3$ on which due to imposed periodicity 3D discrete Fourier transform, F, can be performed using a standard FFT routine. In the discrete Fourier space Eq. (16) can be treated as a linear set of algebraic equations with system matrix M,

$$MA^* = -\delta_d^*, \quad MA^* = -k_F^2 A^* + F\left[k^2 F^{-1}\left(A^*\right)\right], \qquad (17)$$

where the star denotes Fourier image, $A^* = F(A)$ and $k_F{}^2 = k_1{}^2 + k_2{}^2 + k_3{}^2$, where k_j are the Cartesian components of the Fourier wavevector. Despite the matrix M is not provided explicitly, the matrix-vector product can be computed efficiently using the forward and inverse FFT. Hence, we can solve this equation iteratively. In our implementation we use preconditioned GMRES, where the initial guess is provided from the previous time step. We found that a preconditioner, which approximates M with diagonal matrix $M_p = \langle k^2 \rangle - k_F{}^2$, where $\langle k^2 \rangle$ is the value of k^2 averaged over all grid points provides fast enough convergence (usually 2-5 iterations per time step, while for some steps this can go up to 20 iterations or so). We also should note that the treatment of nonlinearities or spatial inhomogeneities (as in Eq. (17)) usually should be stabilized by filtering (dealiasing) procedures. In all such cases we use a standard 2/3 dealiasing rule (zero-padding of the 1/3 of the high frequency Fourier spectrum).

To treat the rest of equations (14) we used explicit time marching schemes (the 6th order Adams-Bashforth-Moulton predictor-corrector initialized by the Runge-Kutta scheme). These equations were treated by two methods, first is the pseudospectral in the Fourier domain (FFT based convolution of the nonlinear terms), and, second, by the Lagrangian tracking of bubbles followed by the particle-in-cell (PIC) particle density estimators, which is a typical approach in many particle physics problems requiring particle-to-grid and grid-to-particle interpolation. The results presented below are obtained using the Lagrangian tracking. It is noticeable that in the numerical experiments we were able to track *all* bubbles in the computational domain, while the number of grid points was much larger than the number of bubbles (e.g. we used 32×32×32 and 64×64×64 grids and a few thousands of bubbles). In fact, this shows that our model, Eqs (3)-(4), should be justified rather using multiple scattering theory (Foldy (1945) [12]) than a two-phase continuum approach [6]. We can remark then that the Bjerknes force in Eq. (6) includes both primary and secondary force, if the first one is due to the incident and the second as due to the scattered field).

The code was also implemented in a 2D version, which physically corresponds to a cylindrical sound source along the z-axis and uniform in the z-direction particle density distribution. As this version is much faster than the 3D version and provides better resolution, it was used in many cases as a fast tool for parametric studies and visualization.

RESULTS

For the initial tests we modeled several typical situations for an air-water system at room conditions and fixed driving frequency 20 kHz. Symmetry (15) was imposed on bubble position and size distributions.

The first situation, which in any case should be considered for understanding, is the case of one-way bubble-field interaction. This is realized when the void fractions α are much smaller than 10^{-6} so from Eq. (4) we have $|k_b|^2 << k_l^2$ and the bubbles do not affect the stationary acoustic filed. In this case the numerical solution simplifies substantially. We have then from Eq. (17)

$$A^* = N_A(k_F^2 - k_l{}^2)\delta_d^*, \quad A = F(A^*), \qquad (18)$$

where N_A is selected to provide the value of maximum $|A|$ be equal to one. Figure 1 illustrates the computed field in 2D for the box size $5\lambda \times 5\lambda$, where $\lambda = 2\pi/k_l$ is the wavelength.

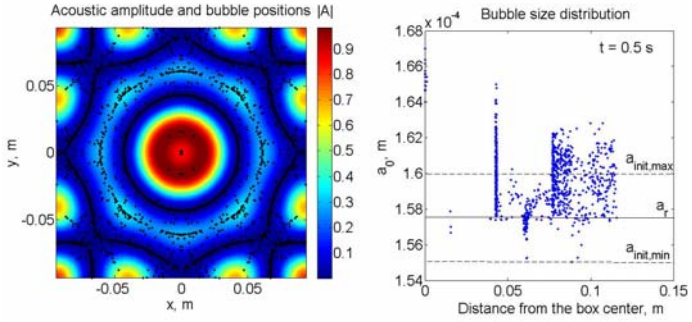

Fig.1. Amplitude of the acoustic field and bubble position and size distribution in 2D standing wave after 0.5 s from the start of sonification. Initial distribution was quasi random in space and in bubble sizes (between $a_{\text{init,min}}$ and $a_{\text{init,max}}$). ε=0.2, 20 kHz, saturated air-water system at 1 bar and T=293 K, one-way interaction.

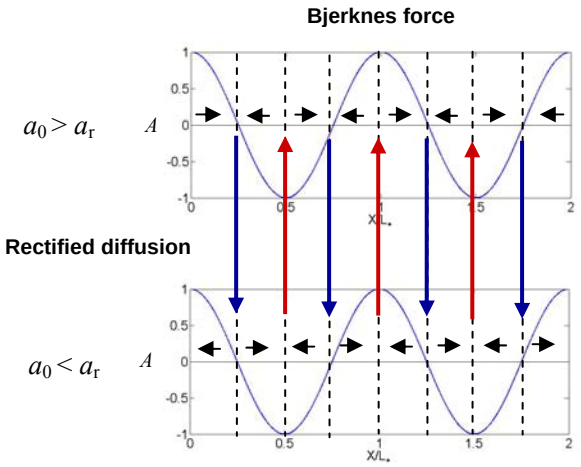

Fig.2. An illustration of Bjerknes force/rectified diffusion instability in a standing wave.

It is well known that due to Bjerknes forces bubbles of subresonance sizes are attracted to the antinodes, while superresonance size bubbles are attracted to the nodes, which

provides strong clustering of the bubbles. However, these attractors are unstable due to the effect of rectified diffusion, since the field near the antinodes is small and bubbles collapse due to surface tension (and also if the liquid is subsaturated). As they become smaller than the resonance size they are pushed out of the antinode by the Bjerknes force. On the other hand, in the nodes bubble grow and when their sizes become larger than the resonance value they are pushed away by the Bjerknes force. Hence, one can observe migration of the bubbles between the attractors. This is illustrated on Fig. 2.

In our simulations we observed that bubbles travel rapidly to the respective attractors and reside there for relatively long time. However, after some time this instability develops and they migrate between the attractors. It is remarkable that relatively small forces (e.g. gravity) play a substantial role in development of this instability, since at the nodes and antinodes of a standing acoustic wave, the Bjerknes force is zero. In the 3D case the structure of the attractors can be much more complicated in terms of geometry and topology. Figure 3 illustrates such attractors for box of size $5\lambda \times 5\lambda \times 5\lambda$. It is seen that these attractors are populated by bubbles and there are very few travelling bubbles (after some sonification time).

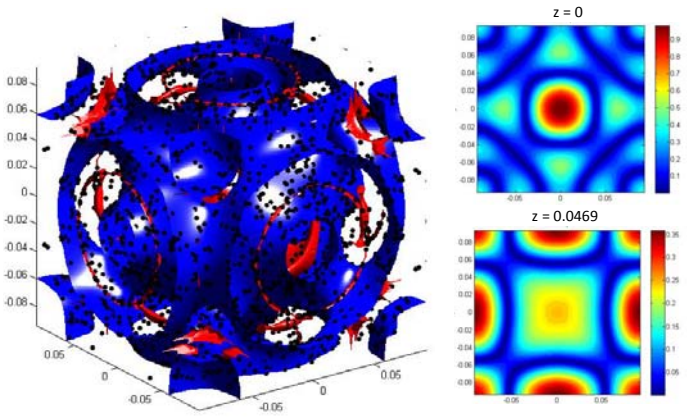

Fig.3. Attractors of a 3D standing wave in a $5\lambda \times 5\lambda \times 5\lambda$ box (the blue surfaces are nodes and the red surfaces and curves are the antinodes) populated by bubbles (the black points) (on the left) and the amplitude of the acoustic field in slices $z = 0$ and $z = 1.25\lambda$ (on the right).

Two-way interaction occurs since bubbles cause strong attenuation and change of the sound speed (and the wavelength) around bubble clusters. Fig. 4 illustrates a scenario, which we observed both in 2D and 3D simulations with initially uniform bubble position and size distributions for the case similar to that on Fig. 1, but with initial void fraction $\alpha \sim 10^{-6}$ -10^{-5}. The initial field is different from that on Fig. 1 due to strong attenuation. Further a self-induced acoustic transparency develops (the source pushes out all bubbles and creates a large region around the source free of bubbles). Then the bubbles travel to the wave nodes (in the present case all bubbles became superresonant by that time) and form filaments (local $\alpha \sim 10^{-4}$ -10^{-3}), which are stable for a long time (but globally unstable, see Fig. 2). Indeed, these bubbles do not affect the field substantially as they are located at the nodes, where the amplitude is zero.

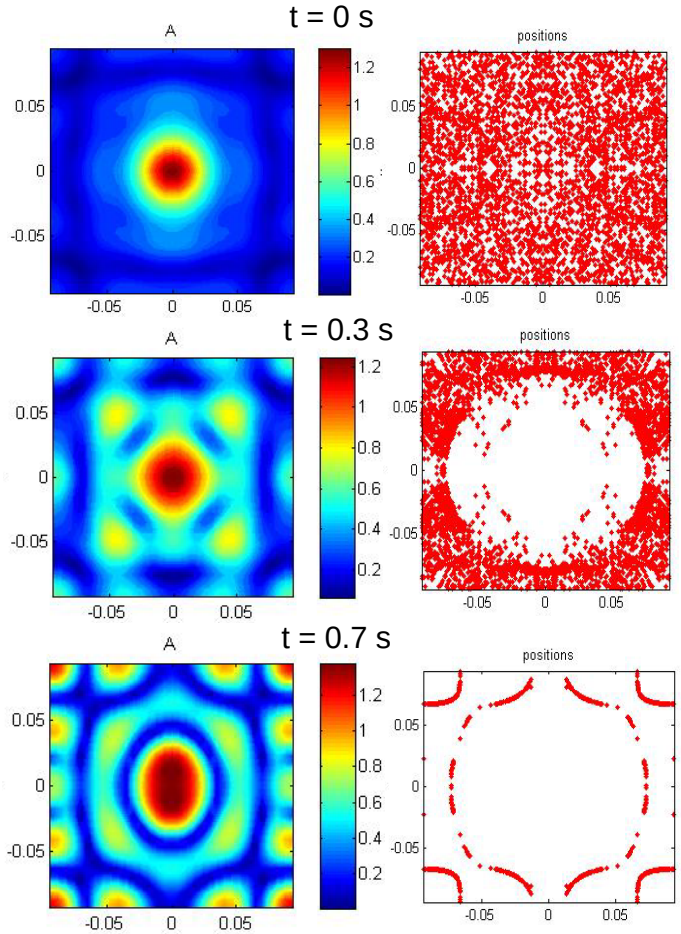

Fig.4. Dynamics of 4000 bubble system with the same parameters as in Fig.1 (but two-way interaction).

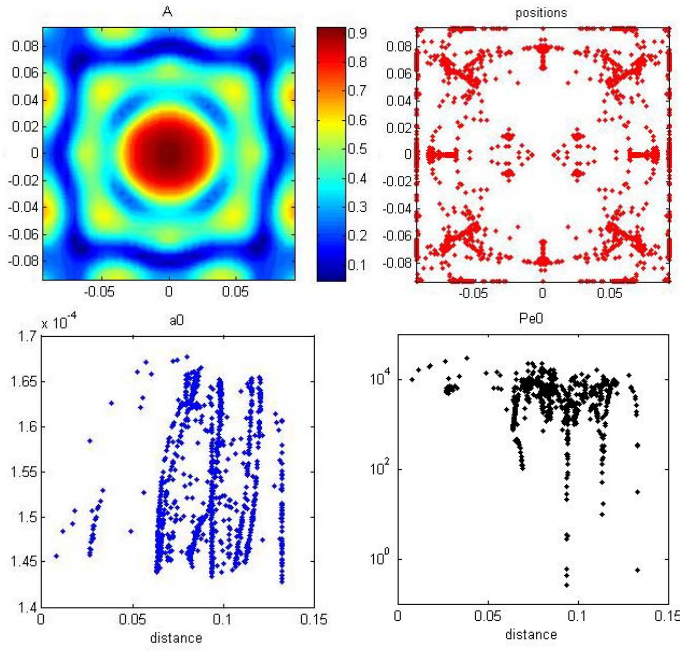

Fig.5. State of the same system as in Fig. 4 at t = 0.7 s but with initial bubble radii distribution between $a_{\text{init,min}}$ and $a_{\text{init,max}} = a_r$ and the same distribution width. The last row of the pictures displays a_0 and Pe_D vs the distance from the box center.

Different patterns can be observed for the same system in the case when initial bubble sizes are just slightly different. Fig. 5 shows that initial distribution of subresonance bubbles develops to a mixed sub/super- resonance bubbles distribution. It is seen that Pe_D can be large or small; in the latter case the neglected transient effects may play a substantial role.

Some results of 3D simulations are displayed in Fig.6. They show that despite the filamentation occurs in the nodes of the wave, the field itself is shaped by the bubbles (the field for different cases is different and it is also different from the field in pure liquid shown in Fig.3). Figure 6 also shows that presumably small effects such as gravity and liquid saturation can be important for self-organization.

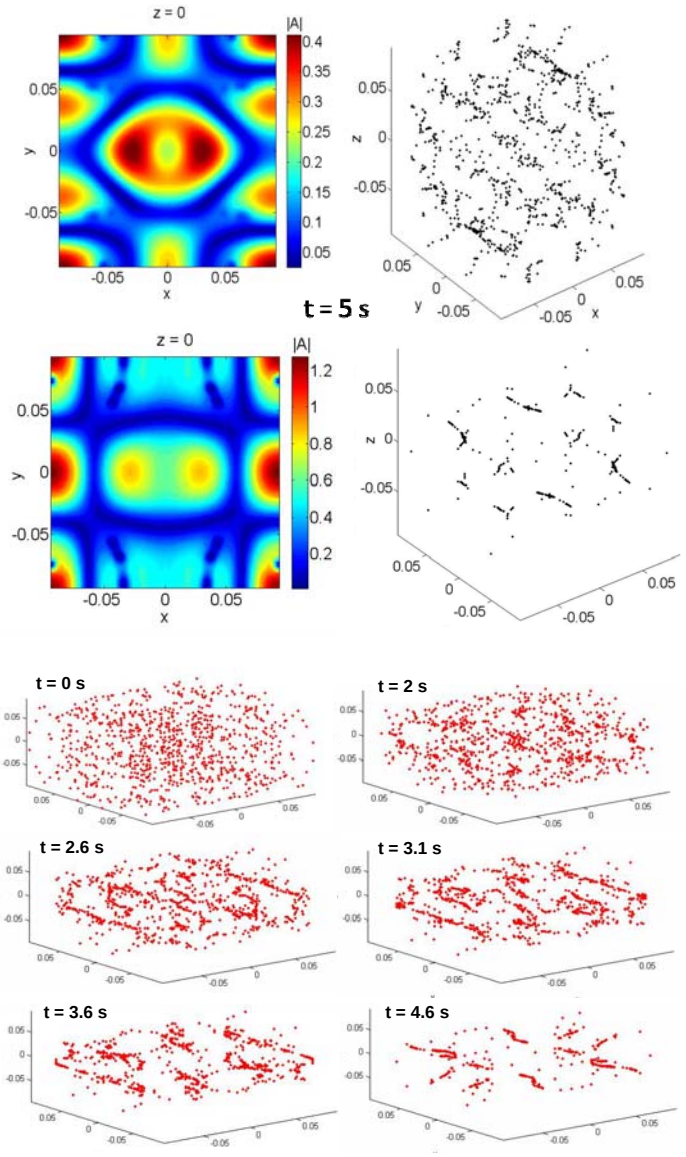

Fig.6. The upper pictures show a slice of the wave amplitude and a bubble pattern in the same box as in Fig. 3 formed during 5 s of sonification for a system of 1000 bubbles with initial size distribution as in Fig.5 for $c_\infty = c_*$ and zero gravity. The next row of pictures correspond to the same case, but for the normal gravity and a subsaturated liquid, $c_\infty = 0.75\ c_*$. The rest of the pictures show stages of the latter pattern development.

CONCLUSION

Preliminary results show that the model and method require substantial parametric studies and comparisons with experiments which are planned as a future work. The numerical method itself shows good enough stability properties and capabilities to solve a complex problem, while for extensive parametric studies high performance computing and optimization of algorithms is required (in our initial implementation one 3D run can take many hours as it may need ~10^5 time steps and, so ~ 10^6 FFTs in 3D). Additional model extensions can be required, which includes accounting for bubble coalescence and fragmentation and modifications accounting for physics of cavitation inception. Equation of rectified diffusion should also be revised substantially to be applicable for the bubbles with translatory motion and transient history, which can be significant for self-organization.

ACKNOWLEDGMENTS

This research is supported by the Grant of the Ministry of Education and Science of the Russian Federation (G34.31.0040).

REFERENCES

[1] Kobelev, Yu.A. and Ostrovsky, L.A. 1989, "Nonlinear acoustic phenomena due to bubble drift in a gas-liquid mixture," *J. Acoust. Soc. Am*, 85, 621-629.

[2] Akhatov, I., Parlitz, U., and Lauterborn, W. 1994, "Pattern formation in acoustic cavitation," *J. Acoust. Soc. Am*, 96, 3627-3635.

[3] Akhatov, I., Parlitz, U., and Lauterborn, W. 1996, "Towards a theory of self-organization phenomena in bubble-liquid mixtures," *Phys. Rev. E*, 54, 3747-3750.

[4] Parlitz, U., Scheffczyk, C., Akhatov, I., and Lauterborn, W. 1995, "Structure formation in cavitation bubble fields," *Chaos, Solitons and Fractals*, 5, 1881-1891.

[5] Gumerov, N.A. 1998 "On self-organization of voids in acoustic cavitation," Proceedings of the Third International Conference on Multiphase Flow, ICMF'98, Lyon, France, paper p512.

[6] Nigmatulin, R.I., 1991 *Dynamics of Multiphase Media.* Vol. 1, 2. Hemisphere, Washington D.C.

[7] Commander, K.W. and Prosperetti, A. 1989 "Linear pressure waves in bubbly liquids: Comparison between theory and experiments," *J. Acoust. Soc. Am.*, 85, 732-746.

[8] Crum, L.A. and Hansen, G.M. 1982 "Generalized equations for rectified diffusion," *J. Acoust. Soc. Am.*, 72, 1586-1592.

[9] Fyrillas, M.M. and Szeri, A.J. 1994, "Dissolution or growth of soluble spherical oscillating bubbles," *J. Fluid Mech.,* 277, 381-407.

[10] Gumerov, N.A. 1996, "The heat and mass transfer of a vapor bubble with translatory motion at high Nusselt numbers," *Int. J. Multiphase Flow,* 22, 259-272.

[11] Levich, V.G. 1959 *Physico-Chemical Hydrodynamics,* Fizmatgiz, Moscow.

[12] Foldy, L.L. 1945, "The multiple scattering of waves," *Phys. Rev.,* 67, 107-119.